

# HYPERSPECTRAL AND MULTISPECTRAL DATA FUSION MISSION ON HYPERSPECTRAL IMAGER SUITE (HISUI)

*Naoto Yokoya and Akira Iwasaki*

Research Center for Advanced Science and Technology, The University of Tokyo, Japan  
yokoya@sal.rcast.u-tokyo.ac.jp

## ABSTRACT

Hyperspectral imager suite (HISUI) is the Japanese next-generation earth-observing sensor composed of hyperspectral and multispectral imagers. Unmixing-based fusion of hyperspectral and multispectral data enables the production of high-spatial-resolution hyperspectral data. HISUI simulated imaging system combining two imagers was developed for verification experiments to investigate the feasibility and clarify the whole procedure of the hyperspectral and multispectral data fusion mission on HISUI. Airborne experiments are planned as simulation tests of HISUI higher-order products. The experimental results of the ground based observation showed the importance of the preprocessing and cross-calibration on the final quality of fused data, which contributes to the practical use of hyperspectral and multispectral data fusion.

**Index Terms**— Hyperspectral and multispectral data fusion, unmixing, hyperspectral imager suite (HISUI)

## 1. INTRODUCTION

Hyperspectral imagers (HSIs) collect approximately 100 to 200 or more spectral bands with 5–10 nm spectral bandwidths, whereas multispectral imagers (MSIs) obtain approximately 4 to 10 spectral bands with larger spectral bandwidths (70–400 nm). HSIs generally have larger ground sampling distance (GSD) than MSIs due to a trade-off of sensor design between spatial and spectral resolutions. Hyperspectral imager suite (HISUI) is the Japanese next-generation earth-observing sensor composed of hyperspectral and multispectral imagers [1]. The GSDs of hyperspectral and multispectral imagers are 30 m and 5 m, respectively. In the visible near infrared spectral range, the HSI has 57 bands, whereas the MSI has 4 bands.

Hyperspectral and multispectral data fusion can produce high-spatial-resolution hyperspectral data [2, 3, 4, 5]. Unmixing-based hyperspectral and multispectral data fusion can enhance the spatial resolution of hyperspectral data with a small spectral distortion [4, 5]. An unmixing-based hyperspectral and multispectral data fusion method, named coupled nonnegative matrix factorization (CNMF), was proposed in

remote sensing [4]. CNMF is composed of alternating unmixing for two images using nonnegative matrix factorization (NMF) [6]. NMF has recently been receiving attention in unmixing of remotely sensed hyperspectral data based on a linear spectral mixture model to deal with severe mixtures considering nonnegativity with simple implementation [7, 8]. A similar approach for resolution enhancement of hyperspectral data using an RGB image was independently proposed in computer vision [5]. This method uses a sparsity promoted unmixing that is suitable for computer vision applications.

Several assumptions for this data fusion are as follows: 1) observing from the same platform with the same observation conditions such as atmospheric and illumination conditions, 2) observing the same scene with accurate image registration, 3) relative sensor characteristics such as spectral response functions (SRFs) and point spread functions (PSFs) are given. Hyperspectral and multispectral data fusion algorithms in remote sensing have mainly been evaluated using synthetic datasets because there is no platform that is composed of hyperspectral and multispectral imagers with the trade-off of spatial and spectral resolution. HISUI will be the first spaceborne platform that satisfies these assumptions. Verification experiments are indispensable to clarify the practical issues and establish the whole operation including the preprocessing and cross-calibration. In this work, we present a high-spatial-resolution hyperspectral imaging system combining hyperspectral and multispectral imagers and show its ground experiment to investigate the feasibility of the hyperspectral and multispectral data fusion mission on HISUI. The plan of airborne experiments is also described as further simulation tests.

## 2. UNMIXING-BASED HYPERSPECTRAL AND MULTISPECTRAL DATA FUSION

### 2.1. The CNMF algorithm

In this work, CNMF is used for HISUI hyperspectral and multispectral data fusion mission owing to its advantage for remote sensing data. The aim of hyperspectral and multispectral data fusion is to estimate unobservable high-spatial-resolution hyperspectral data ( $\mathbf{Z} \in \mathbb{R}^{L_h \times P_m}$ ) from observable

low-spatial-resolution hyperspectral data ( $\mathbf{X} \in \mathbb{R}^{L_h \times P_h}$ ) and high-spatial-resolution multispectral data ( $\mathbf{Y} \in \mathbb{R}^{L_m \times P_m}$ ) (Fig. 1).  $L_h$  and  $L_m$  denote the numbers of spectral channels of hyperspectral and multispectral sensors, respectively.  $P_h$  and  $P_m$  denote the numbers of pixels of hyperspectral and multispectral images, respectively. All data are expressed in matrix form with each column vector representing a spectrum at each pixel.  $L_h > L_m$  and  $P_h < P_m$  are satisfied by the trade-off between spectral and spatial resolutions. Hyperspectral and multispectral data can be seen as degraded datasets of the ideal data in spatial and spectral domains:

$$\mathbf{X} = \mathbf{Z}\mathbf{S} \quad \text{and} \quad \mathbf{Y} = \mathbf{R}\mathbf{Z}, \quad (1)$$

where  $\mathbf{S} \in \mathbb{R}^{P_m \times P_h}$  and  $\mathbf{R} \in \mathbb{R}^{L_m \times L_h}$  are the relative PSF and SRF matrices, respectively. With the linear spectral mixture model, high-spatial-resolution hyperspectral data can be expressed as

$$\mathbf{Z} \approx \mathbf{E}\mathbf{A}, \quad (2)$$

where  $\mathbf{E} \in \mathbb{R}^{L_h \times D}$  and  $\mathbf{A} \in \mathbb{R}^{D \times P_m}$  denote the endmember and abundance matrices, respectively, and  $D$  is the number of endmembers. The high-spatial-resolution hyperspectral data can be obtained by estimating the endmember and abundance matrices from observed two datasets. First, the algorithm starts from NMF-based unmixing of the hyperspectral data to estimate the endmember spectra taking its spectral advantage. Next, the multispectral data is unmixed by NMF after initializing the endmember and abundance matrices using the unmixing results of the hyperspectral data. The sequential unmixing for hyperspectral data is processed after initializing the abundance fractions by using the unmixing results of the multispectral data. After that, two data are alternately unmixed until convergence and the fused data can be obtained by multiplying the endmember matrix by the high-spatial-resolution abundance matrix. NMF converges to a local minimum; therefore, the initialization is important. The relative SRFs are used for initializing the endmember spectra in the multispectral unmixing and the relative PSF is used for initializing the abundance maps in the hyperspectral unmixing. CNMF uses the advantages of hyperspectral and multispectral data, i.e., spectral and spatial resolutions, respectively, to find better local minima of the other unmixing process. More details about the CNMF method are given in [4].

## 2.2. Preprocessing and cross-calibration

When applied to real datasets, the preprocessing of observed data and the cross-calibration of the two sensors are necessary to satisfy the assumptions [9]. Fig. 2 shows a flowchart of the whole process. First, the observed datasets are radiometrically corrected and co-registered in the preprocessing. Accurate image registration is critical to consistency of abundance maps between hyperspectral and multispectral images. Histogram matching is useful for radiometric correction. Extreme noise contained in the data need to be corrected

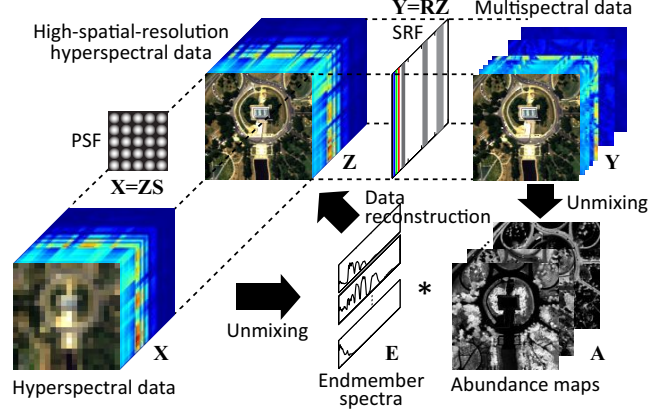


Fig. 1. Illustration of unmixing-based hyperspectral and multispectral data fusion

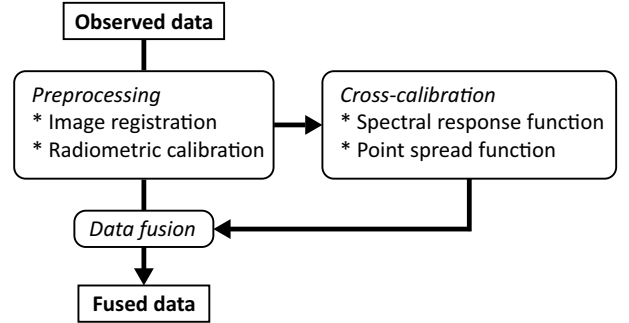
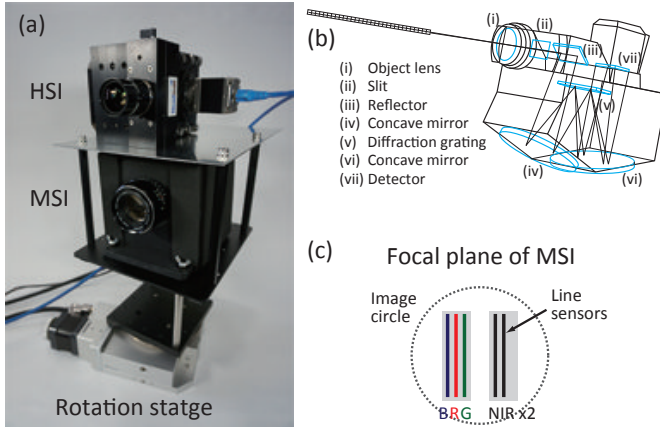


Fig. 2. Flowchart of hyperspectral and multispectral data fusion

in the preprocessing because it can be detected as one of endmembers and worsen unmixing results and a quality of fused data. Next, the cross-calibration is performed to obtain relative sensor characteristics, such as SRF and PSF. The relative SRFs, which are used for the initialization of the endmember spectra of the multispectral unmixing, can be estimated by constrained least squares methods that is solved by quadratic programming [9, 10]. The relative PSF is obtained by comparing sharpnesses of hyperspectral and multispectral images and used for the initialization of the abundance maps of the hyperspectral unmixing. Finally, the alternate unmixing of hyperspectral and multispectral data is processed using the relative sensor characteristics for relating endmember spectra and abundance fractions.

## 3. GROUND EXPERIMENT

We carried out the ground experiment of hyperspectral and multispectral data fusion using combined imagers as shown in Fig. 3(a). The HSI is HyperSpec-VNIR-C of Headwall photonics Inc., which uses a diffraction grating spectrometer as illustrated in Fig. 3(b). This sensor can observe spectral images in 12 bit over the range of 390–1040 nm with the



**Fig. 3.** (a) Combined optical imagers and illustrations of (b) HSI and (c) focal plane of MSI.

1.29 nm spectral resolution. The detector originally has the  $1024 \times 1392$ -pixel size in the spectral and spatial directions; however, a spectral image is recorded using binning to improve the frame rate and signal-to-noise ratio, which results in the  $512 \times 696$ -pixel size. To simulate HISUI specifications, the spectral sampling distance is downsampled as 10.34 nm with 64 channels. The MSI is a prototype of HODOYOSHI-1, which is the Japanese earth-observing micro-satellite. It has a 4-channel line-scanning system with the 4120-pixel-size line detector. Since the four line detectors are located in parallel positions on the focal plane as shown in Fig. 3(c), four bands images have disparities in the scanning direction. We use an image matching technique to register them by shifting.

The two imagers were set up in parallel planes to align the cross-track directions and observe a landscape using a rotating stage. First, sub-images are extracted and spatially co-registered using image matching assuming that captured objects are relatively far enough from the observation locations comparing with the distance between the centers of focal planes. The RGB image of multispectral data is shown in the left-side of Fig. 5. The difference of spatial sampling distance is 6-fold, which is the same ratio of the GSDs of HISUI between hyperspectral and multispectral imagers. The two datasets were radiometrically modified and converted into reflectance using a spectralon target of Labsphere, Inc.. Next, the relative SRFs were estimated using only observed datasets and the prior knowledge for the spectral ranges. We used the constrained least squares method, which considers smoothness and nonnegativity [10]. Fig. 4 shows the estimated relative SRFs of 4 channels. Although we used only observed datasets, the results are consistent with the pre-measured SRFs of detectors, which indicates that the onboard cross-calibration is useful even when the sensor characteristics are unknown or changed on orbit. In the case of HISUI, the prelaunch SRFs can be used for the constraints to estimate the relative SRFs on orbit [9]. Finally, we applied the

**Table 1.** SAE (in degrees) and PSNR (in decibels).

	HSI	MSI
SAE	1.483	0.937
PSNR	31.62	42.81

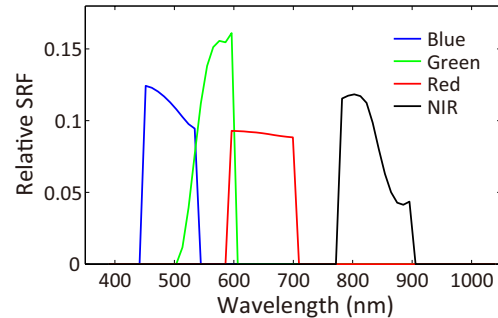


**Fig. 5.** Estimated relative SRFs.

CNMF method to the datasets using the relative SRFs and PSF. Fig. 5 shows two zoomed views of the hyperspectral and fused images in the 483 and 710 nm ranges. As shown in the zoomed images, highly detailed spatial information is acquired for the hyperspectral image.

Since the high-spatial-resolution hyperspectral data is not available, the quality of the fused data is evaluated by comparing hyperspectral and multispectral images degraded from the fused image with the original input images for evaluating that the fused image inherits the information both in the hyperspectral and multispectral images. The spectral angle error (SAE) and the peak signal-to-noise ratio (PSNR) were used to calculate the spectral and spatial reconstruction qualities, respectively. Table 1 summarizes the average SAE and PSNR. The evaluation results of the multispectral data is relatively better than that of the hyperspectral data. The SAE is calculated at each pixel and the PSNR is computed for each band image; therefore, the spatial information has a large impact on both criteria. Since the spatial information of the fused data, i.e., the abundance maps were obtained from the multispectral unmixing, the fused data was biased to the multispectral data in spatial domain, which results in the better evaluation results with the multispectral data. Errors of the degraded hyperspectral data are due to the misregistration between the hyperspectral and multispectral images, which is caused by the difference of viewing angle and optical-system aberrations and misalignments. It indicates that accurate registration of the two images is essential to obtain high-quality fused data.

#### 4. AIRBORNE SIMULATION

Airborne simulation tests for the hyperspectral and multispectral data fusion mission on HISUI will be carried on August in 2013 and 2014. The study area is the Tama forest sci-

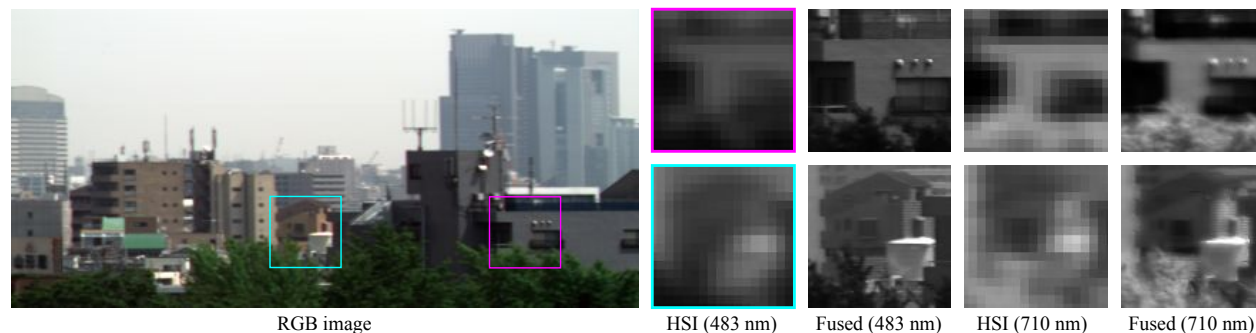


**Fig. 4.** RGB image of multispectral data and two zoomed sub-images of hyperspectral and fused data in 483 and 710 nm.

ence garden in Tokyo, Japan. Hyperspectral and multispectral imaging sensors are mounted on the same platform to satisfy the assumption of the same observation conditions. The HSI is the same imager with the ground experiment. The GSD is 2.5 m and the swath width is 750 m. The prototype of HODOYOSHI-1 and EOS 5D Mark II of Canon Inc. will be mounted as MSIs. EOS 5D Mark II captures 3 spectral channels, i.e., red, green, and blue, in 14 bit with the 0.25 m GSD and the 750 m swath width. The hyperspectral sensor is a pushbrooming imager; however, one of the multispectral sensors is with a 2D image capturing. Therefore, image registration is significant. HISUI simulation datasets will be synthesized to evaluate hyperspectral and multispectral data fusion and to investigate its effectiveness for tree species classification.

## 5. CONCLUSION

We developed a high-spatial-resolution hyperspectral imaging system combining hyperspectral and multispectral sensors and presented the ground experiment for the hyperspectral and multispectral data fusion mission on HISUI. The whole process of data fusion including the preprocessing and cross-calibration was clarified and the feasibility of this mission was investigated. The preprocessing and cross-calibration are important for the final quality of fused data satisfying the assumptions of data fusion. We explained the plan of airborne experiments for further simulation tests. This work contributes to the practical use of hyperspectral and multispectral data fusion, which can be the prototype trial for the higher-order product of the HISUI datasets.

## 6. ACKNOWLEDGEMENT

This work was supported by contract with the National Institute of Advanced Industrial Science and Technology (AIST) and KAKENHI (24360347).

## 7. REFERENCES

- [1] N. Ohgi, T. Kawashima A. Iwasaki, and H. Inada, "Japanese hyper-multi spectral mission," in *Proc. IEEE IGARSS 2011*, 2011.
- [2] R. C. Hardie, M. T. Eismann, and G. L. Wilson, "Map estimation for hyperspectral image resolution enhancement using an auxiliary sensor," *IEEE Transactions on Image Processing*, vol. 13, no. 9, pp. 1174–1184, September 2004.
- [3] M. T. Eismann and R. C. Hardie, "Application of the stochastic mixing model to hyperspectral resolution enhancement," *IEEE Transactions on Geoscience and Remote Sensing*, vol. 42, no. 9, pp. 1924–1933, September 2004.
- [4] N. Yokoya, T. Yairi, and A. Iwasaki, "Coupled nonnegative matrix factorization unmixing for hyperspectral and multispectral data fusion," *IEEE Transactions on Geoscience and Remote Sensing*, vol. 50, no. 2, pp. 528–537, February 2012.
- [5] R. Kawakami, J. Wright, Y.-W. Tai, Y. Matsushita, M. Ben-Ezra, and K. Ikeuchi, "High-resolution Hyperspectral Imaging via Matrix Factorization," *Proceedings of the 2011 IEEE Conference on Computer Vision and Pattern Recognition*, pp. 2329–2336, 2011.
- [6] D. D. Lee and H. S. Seung, "Learning the parts of objects by non-negative matrix factorization," *Nature*, vol. 401, pp. 788–791, October 1999.
- [7] L. Miao and H. Qi, "Endmember extraction from highly mixed data using minimum volume constrained nonnegative matrix factorization," *IEEE Trans. Geosci. Remote Sens.*, vol. 45, no. 3, pp. 765–777, Mar. 2007.
- [8] S. Jia and Y. Qian, "Constrained nonnegative matrix factorization for hyperspectral unmixing," *IEEE Trans. Geosci. Remote Sens.*, vol. 47, no. 1, pp. 161–173, Jan. 2009.
- [9] N. Yokoya, N. Mayumi, and A. Iwasaki, "Cross-calibration for data fusion of EO-1/Hyperion and Terra/ASTER," *IEEE Journal of Selected Topics in Applied Earth Observations and Remote Sensing*, in press, 2013.
- [10] G. D. Finlayson, S. Hordley, and P. M. Hubel. "Recovering device sensitivities with quadratic programming," *Proceedings of the IS and T/SID Sixth Color Imaging Conference: Color Science, Systems, and Applications*, pp. 90–95, November 1998.